Journal of Statistical Physics, Vol. 70, Nos. 3/4, 1993

Time Evolution of the Probability Distribution in Stochastic and Chaotic Systems with Enhanced Diffusion

Rosario Nunzio Mantegna[1]

Received February 28, 1992; final June 8, 1992

We perform a detailed study of the time evolution of the probability distribution for two processes displaying enhanced diffusion: a stochastic process named the Lévy walk and a deterministic chaotic process, the amplified climbing-sine map. The time evolution of the probability distribution differs in the two cases and carries information which is peculiar to the investigated process.

KEY WORDS: Random walks; Lévy walks; anomalous diffusion; stable distributions.

1. INTRODUCTION

In recent years, many studies has been devoted to dynamical processes displaying anomalous diffusion.[1-5] In these processes the mean square displacement $\langle r^2(t) \rangle$ shows a time dependence which differs from the linear dependence $\langle r^2(t) \rangle \propto t$ observed for the simple Gaussian Brownian motion.[3,6] Anomalous diffusion is characterized by

$$\langle r^2(t) \rangle \propto t^m \tag{1}$$

with $m \neq 1$. A subdiffusive behavior (i.e., $m < 1$) has been observed in systems with geometric constrains (disordered systems,[1] diffusion in convective rolls,[7] fractals,[4] etc.), whereas enhanced diffusion ($m > 1$) is typical for intermittent dynamical systems[8-10] and turbulence.[11,12] Apart from the turbulence, enhanced diffusion has been also detected in polymer-like[13] and economic[14] systems.

[1] Istituto di Fisica dell'Università, I-90123 Palermo, Italy.

822/70/3-4-14

In this paper we report a detailed study on the time evolution of the probability $P(r, t)$ that a particle is at position r at time t for two different physical models displaying enhanced diffusion. The first is a stochastic model named the Lévy walk,[2, 15, 16] while the second is a chaotic system, the amplified climbing-sine map.[9] Both models were originally proposed to describe fully developed turbulence. The study of the time evolution of the probability $P(r, t)$ is relevant for processes displaying anomalous diffusion. In fact, for processes with normal diffusion the $P(r, t)$ distribution is expected to be Gaussian, while in the presence of anomalous diffusion a large variety of distributions can be observed. In the presence of anomalous diffusion we can have Lévy distributions[3,6,17,18] or we can observe Gaussian distributions with the variance growing more than linearly with time[19,20] or a leptokurtic probability distribution with fine structure for a chaotic intermittent diffusive evolution.[8–10] In all these cases the probability distributions carry information which is peculiar to the model investigated. The knowledge of these peculiarities for the different models can help in the interpretation of experimental data showing enhanced diffusion. In this paper, our main aim is to show that a detailed analysis of the time evolution of the probability distribution provides useful information for the identification of the model better describing a set of experimental data displaying enhanced diffusion. In particular we show the probability $P(r, t)$ is different for the two studied processes, especially in the important region $P(0, t)$, even if the mean square displacement shows the same time dependence.

In the next section we study, in detail, the time evolution of the probability distribution of the stochastic process named the Lévy walk in the presence of enhanced diffusion. In Section 3 we perform a similar analysis on the time evolution of the probability distribution of the amplified climbing-sine map. We discuss and compare the obtained results in the last section.

2. LÉVY WALKS

A Brownian motion for which the probability distribution $P(r, t)$ is a Lévy[3,6,17,18] (or stable) non-Gaussian distribution for every r and t is called a Lévy flight.[18] A stable distribution of index α is the probability distribution of any linear combination of n independent random variables x_n, each of them characterized by the same probability distribution $p(x)$ decreasing as $x^{-(1+\alpha)}$ for large x, when n tends to infinity. Lévy showed that this property, familiar for Gaussian variables (stable distribution characterized by $\alpha = 2$), is in fact valid for a wider ensemble of stochastic variables (characterized by $0 < \alpha < 2$) if one releases the hypothesis of finite

second moment.[17] The Lévy distribution can be symmetrical or asymmetrical, depending on a control parameter. In this paper for the sake of simplicity we deal only with symmetrical Lévy distributions. Symmetrical Lévy distributions with zero mean are defined by

$$P_\alpha(r, t) = \pi^{-1} \int_0^\infty \exp(-\gamma_1 t k^\alpha) \cos(kr)\, dk \tag{2}$$

The parameter α characterizes the Lévy distribution, while γ_1 defines the time scale. Apart from the case $\alpha = 2$ (Gaussian distribution), a Lévy distribution of order α has moments $\langle r^n \rangle$ diverging for $n > \alpha$. For this reason Lévy flights have second moment diverging at every time $\langle r^2(t) \rangle = \infty$.

Lévy walks are stochastic processes where spatial jumps of arbitrary length (as for Lévy flights) are allowed but long steps are penalized by requiring a longer time to be performed. This is achieved by imposing a spatiotemporal coupling in the probability $\phi(r, t)$, i.e., the probability density that a transition displacement r occurs at a time t after the previous transition. A suitable function is[21, 22]

$$\phi(r, t) = A r^{-\mu} \delta(r - t^\nu) \tag{3}$$

The presence of a coupled spatiotemporal memory makes it possible to observe the second moment at finite times. Moreover, for a wide interval of the control parameters μ and ν this process shows enhanced diffusion.[2,21,22] Below we present the results of our numerical simulations of Lévy walks characterized by the spatiotemporal coupling memory of Eq. (3). We perform numerical simulations in one dimension by following the procedure proposed in ref. 21. The time evolution of the walker $r(t)$ is obtained by generating a random distance r distributed as

$$\phi(r) = \int_0^\infty dt\, \phi(r, t) = C r^{-(\mu + 1 - 1/\nu)} \tag{4}$$

and imposing that the time needed to travel this distance is given by $t = |r|^{1/\nu}$ in agreement with Eq. (3). A typical realization of the process (characterized by $\mu = 2.0$ and $\nu = 1.5$) is given in Fig. 1. By studying the time evolution of the mean square displacement $\langle r^2(t) \rangle$ for $\nu = 1.5$ and for several values of the control parameter μ belonging to the range $[1, 4]$ we observe, in agreement with previous studies,[21] the mean square displacement $\langle r^2(t) \rangle$ proportional to t^m with m greater than 1 for $\mu < (1 + 2\nu)/\nu$ ($\mu < 2.66$ for $\nu = 1.5$). The results of our investigations are collected in Fig. 2. After the check that the system displays enhanced diffusion for an appropriate choice of the control parameters, we study in detail the line

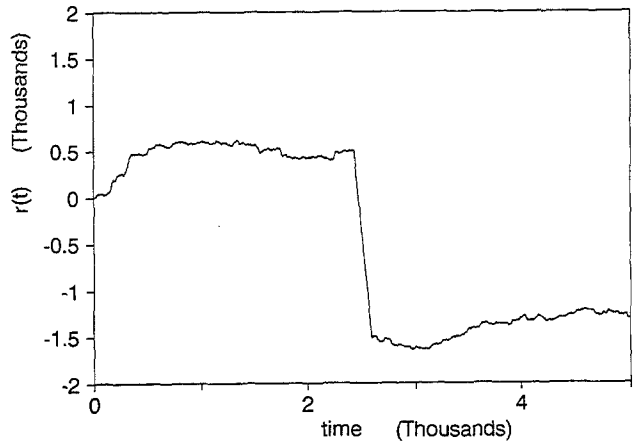

Fig. 1. Single realization of the time evolution of the one-dimensional Lévy walk characterized by $\mu = 2.0$ and $\nu = 1.5$.

shape of the probability distribution $P(r, t)$ as a function of the control parameter μ at different times. Our results show that the central part of $P(r, t)$ has a Lévy shape for $2/\nu < \mu < (1 + 2\nu)/\nu$ even for finite times and moreover the convergence to the Lévy shape is higher for longer times in the wings of distributions. In Fig. 3 we show the $P(r, t)$ observed for $\mu = 2.0$

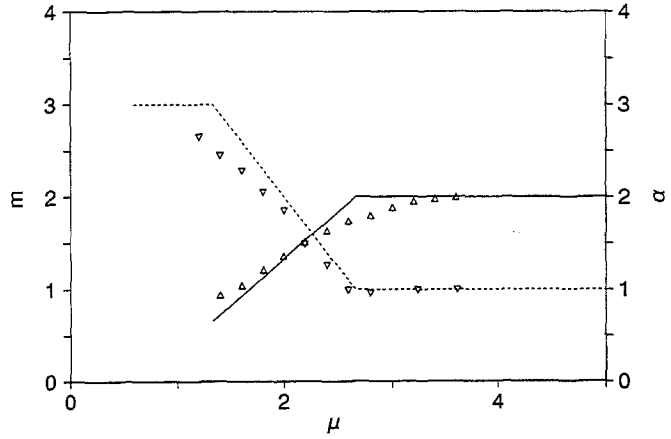

Fig. 2. Lévy walks simulated for $\nu = 1.5$ and for several different values of the control parameter μ. The diffusion exponent m of the mean square displacement (∇) and the order α of the Lévy stable distribution ($\triangle$) describing the central region of the probability distribution are given as a function of the control parameter μ. The dashed line is the theoretical prediction for the diffusion exponent obtained in ref. 21 [Eq. (13)] and the full line is the plot of Eq. (9). Both curves are plotted for $\nu = 1.5$.

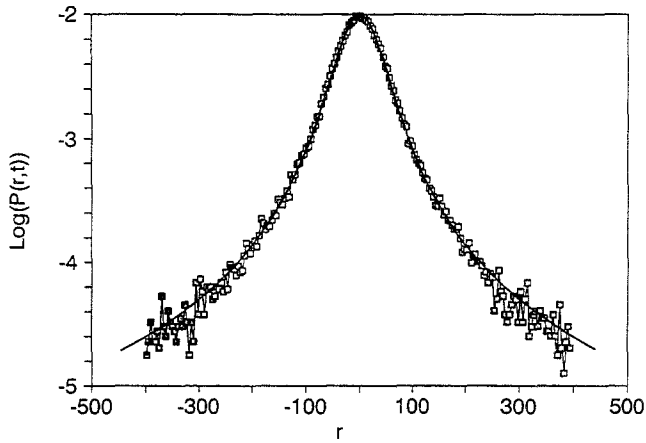

Fig. 3. Logarithm of the probability distribution (□) obtained by collecting 10^5 different realizations of a Lévy walk characterized by $\mu = 2.0$, $\nu = 1.5$, and $t = 100$. The full line is a Lévy stable distribution with $\alpha = 1.36$ and $\gamma_1 t = 100$. The agreement between the two curves is very good for more than two decades from the maxima of the curves.

and $\nu = 1.5$ at $t = 100$. The distribution function is obtained by analyzing the time evolution of 10^5 different realizations. In the same figure we report a Lévy stable distribution of order $\alpha = 1.36$ and $\gamma_1 t = 100$ (see below for the determination of the parameters α and γ_1). The agreement between the two curves is quite remarkable, especially in the central part of the distribution.

In our simulations, for each value of the parameter μ we collect a set of $P(r, t)$. The collection of a sufficient number of $P(0, t)$ allows us the determination of the characterizing parameter α with an high degree of accuracy. The method is the following: we hypothesize that a large part of the probability distribution of our process is well described by a Lévy shape (Fig. 3) and we observe that for Lévy distributions

$$P_\alpha(0, t) = \frac{\Gamma(1/\alpha)}{\pi\alpha(\gamma_1 t)^{1/\alpha}} \tag{5}$$

where $\Gamma(x)$ is the gamma function and γ_1 is a parameter characterizing the distribution $P_\alpha(0, 1)$. The time dependence of $P_\alpha(0, t)$ is a power-law dependence for Lévy distributions [Eq. (5)]. Under this hypothesis, by studying the time evolution of $\log(P(0, t))$ as a function of $\log(t)$, we can obtain the parameter α characterizing the process for the selected values of the control parameters μ and ν. In Fig. 4 we show a log-log plot of $P(0, t)$ as a function of time for a Lévy walk characterized by $\mu = 2.0$ and $\nu = 1.5$. From the plot it is evident that the time dependence of $P(0, t)$ is a power-

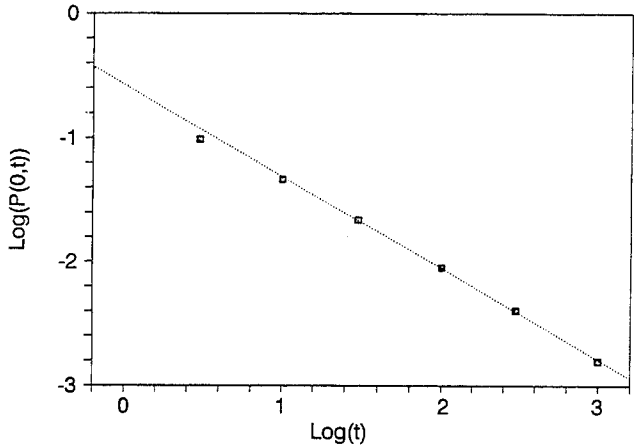

Fig. 4. Log-log plot of the probability of returning to the origin $P(0, t)$ as a function of the time for a Lévy walk ($\mu = 2.0$, $\nu = 1.5$). Squares are the results of simulation (10^5 realizations) and the dotted line is the best linear fitting of the last five points. From the slope ($slope = -0.735$) of the linear fitting we obtain the value of the parameter α ($\alpha = -1/slope = 1.36$) characterizing the simulated Lévy walk.

law dependence after a brief period of time (ensuring convergence of the central part of the distribution to a Lévy shape). From the log-log plot of the $P(0, t)$ data we determine the parameter α by best linear fitting of the data (Fig. 4). The γ_1 parameter is obtained by solving Eq. (5) with the obtained value of α at a time t^* ensuring the convergence of the central part of the distribution $P(0, t^*)$ to a Lévy shape. The values of the parameters α and γ_1 obtained by this procedure are then used to describe the entire $P(r, t)$ for each family of simulations. With this test we check the validity of the assumption of Lévy shape used to write down Eq. (5). In this analysis the parameter γ characterizing a distribution at the time t is related to the parameter γ_1 through the relation $\gamma = \gamma_1 t$ [Eq. (2)]. We are able to describe with only α and γ_1 parameters and with an increasing accuracy in time the entire set of probability distributions $P(r, t)$ obtained by simulating the process for the selected couple of values of the control parameters μ and ν (Fig. 5a). The agreement between the simulated $P(r, t)$ and the calculated $P_\alpha(r, t)$ is quite remarkable over a wide range of the variable r around the origin (Fig. 5a). This result clearly show that the hypothesis that the central part of the probability distribution is well described by a Lévy distribution is a good hypothesis.

The values of the parameter α obtained by this procedure are showed in Fig. 2. In our simulations we set $\nu = 1.5$ and we investigate the behavior of the Lévy walks for several different values of the parameter μ. Our

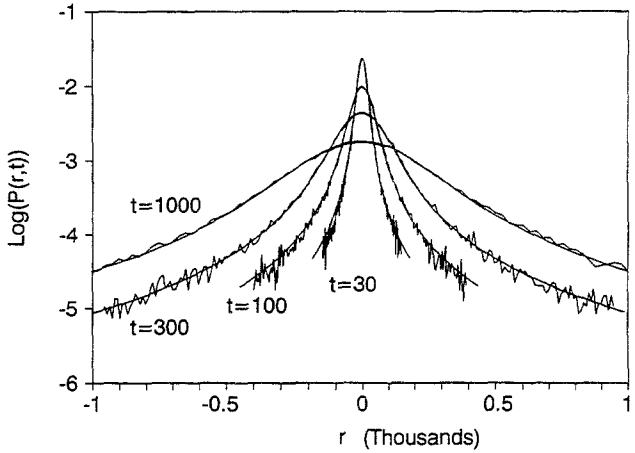

(a)

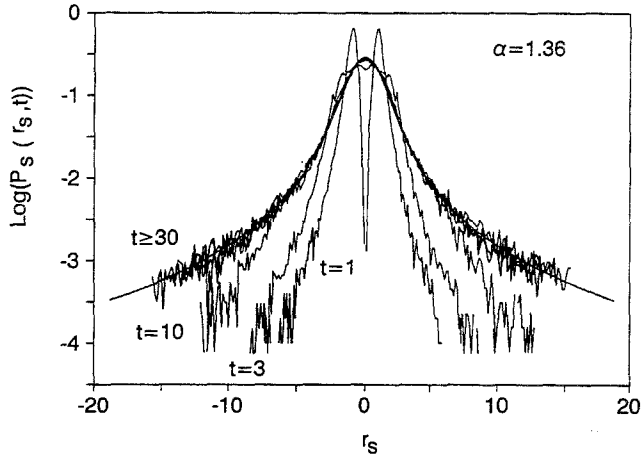

(b)

Fig. 5. Lévy walk characterized by $\mu = 2.0$ and $\nu = 1.5$. (a) Family of probability distributions obtained at different times ($t = 30$, 100, 300, and 1000). Noisy lines are the results of simulation (10^5 realizations), while smooth lines are Lévy stable distributions of order $\alpha = 1.36$ and $\gamma = \gamma_1 t$ with $\gamma_1 = 1.00$. The plot is logarithmic to evidence the behavior of the wings of distributions. The agreement between simulated distributions and Lévy distributions of order $\alpha = 1.36$ is excellent in the investigated spatial range. (b) The same probability distributions as in (a) plus the distributions observed for $t = 1$, 3, and 10 presented in scaled units, $r_s = r/t^{1/\alpha}$ and $P_s(r_s, t) = t^{1/\alpha} P(r_s, t)$. The distributions converge to the Lévy distribution of order $\alpha = 1.36$ (full smooth line) for $t \geqslant 30$ in the investigated range of the scaled position $[-16, 16]$. Moreover, the probability distributions obtained for $t = 1$, 3, and 10 display wings each of which is decreasing more rapidly than expected for the Lévy distribution of order α.

method also provides a way to study the convergence in time of the distribution $P(r, t)$ to a Lévy distribution $P_\alpha(r, t)$. We observe that Lévy stable distributions follow the scaling relation

$$P_\alpha(t^{1/\alpha} r, \gamma_1 t) = \frac{P_\alpha(r, \gamma_1)}{t^{1/\alpha}} \tag{6}$$

so that the study of the convergence to a Lévy shape is facilitated if we plot $P(r, t)$ in the scaled units $r_s = r/t^{1/\alpha}$ and $P_s(r_s, t) = t^{1/\alpha} P(r_s, t)$. After the determination of the parameter α for each family of probability distributions, we plot each set of distributions in terms of the defined scaled units. A family of scaled probability distributions is showed in Fig. 5b. It is the same family already plotted in Fig. 5a with in addition the probability distributions observed for $t = 1$, 3, and 10. From the figure we note that the probability distribution converges quite quickly to the Lévy distribution of order $\alpha = 1.36$ (smooth line in the scaled plot) in the central part, whereas the convergence on the wings is observed for longer times. Our numerical results show also that the convergence is quicker for processes characterized by higher values of the parameter α.

We interpret our numerical results by using some theoretical results presented in ref. 22. In ref. 22 the authors show that the Laplace–Fourier transform of the stepping probability [Eq. (3)]

$$\phi(k, u) = A \sum_r \int_0^\infty dt\, e^{-ikr - ut} \delta(r - t^\nu)\, r^{-\mu} \tag{7}$$

in the region $k \gg u$ can be expressed for $\mu\nu > 2$ as

$$\phi(k, u) = 1 - C_1 u - C_2 k^\alpha \tag{8}$$

with

$$\alpha = \min((\mu\nu - 1)/\nu, 2) \tag{9}$$

and with C_1 and C_2 constant. From this result, by using the formalism of continuous-time random walk,[23] it can be shown that the Laplace–Fourier transform of the probability $P(r, t)$, $\rho(k, u)$ for $k \gg u$ and $\mu\nu > 2$, is given by

$$\rho(k, u) \propto \frac{1}{u + Ck^\alpha} \tag{10}$$

This shows that our numerical results are in agreement with the theory developed in ref. 22, because (10) is the Laplace–Fourier transform of a

Lévy probability distribution of order $\alpha = \min((\mu v - 1)/v, 2)$. In Fig. 2 we show as a full line this theoretical dependence between the parameter α and the control parameter μ for $v = 1.5$ [Eq. (9)]. The agreement between theory and numerical results is remarkable even if the decrease of α is considerably smoother than theoretically expected in the transition between the Gaussian ($\alpha = 2$) and Lévy ($\alpha < 2$) regimes. It is worth noting that we determine the parameter α by investigating the central part, $P(0, t)$, of the probability distribution; due to this our technique gives a higher accuracy with respect to the analyses performed by investigating the wings of the probability distribution, especially for analyses of sets of realizations that are moderately small. Moreover, our numerical observations about the convergence of a Lévy walk on a Lévy flight are also in agreement with the theoretical predictions presented in the literature[22]; in support of this statement we recall that (10) is valid under the assumption $k \gg u$. This condition is verified for a wider interval of the variable k for longer times.

3. AMPLIFIED CLIMBING-SINE MODEL

In this section we present a study of the time evolution of the probability distribution $P(r, t)$ of a chaotic model, the amplified climbing-sine map.[9,24] The investigated map generates a diffuse process with the variance growing asymptotically like t^m with $m \geqslant 1$. This chaotic model shows enhanced diffusion for wide ranges of the control parameters. An enhanced diffusion behavior, characteristic of turbulent diffusion, can then also be generated by an intermittent dynamical chaotic mechanism.[9] We focus our attention on the time evolution of the probability distribution $P(r, t)$ to check if enhanced diffusion is associated with a Lévy distribution in this chaotic model. Below we will show that the probability distribution is leptokurtic. In addition the shape of the probability distribution differs from the Lévy shape greatly in the region close to the origin $P(r \approx 0, t)$. The one-dimensional amplified climbing-sine map is

$$r_{t+1} = r_t + a\,|r_t|^p \sin(r_t) \tag{11}$$

where a and p are the control parameters. As in previous studies,[9,24] in our simulations the control parameter p falls in the range $0 < p < 2/3$ and we choose the control parameter a higher than the critical value for the onset of diffusion and lower than the value at which the flip bifurcation takes place in the first cells $(-2\pi, 0)$ and $(0, 2\pi)$.[9] Different realizations of the process are obtained by selecting randomly the initial condition r_0 within the interval $[-0.5, 0.5]$. In Fig. 6 we show a single realization of the process obtained for $a = 3.75$ and $p = 0.5$. In the figure we also show an

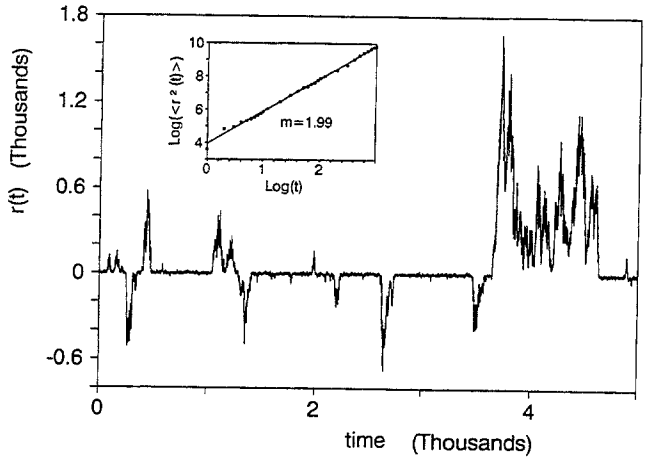

Fig. 6. Amplified climbing-sine map, single realization of the chaotic time evolution characterized by $a = 3.75$ and $p = 0.5$. An intermittent behavior of the time evolution is evident. In the inset we show the time evolution of the mean square displacement of the process obtained by analyzing an ensemble of 10^4 different realizations for the same values of the control parameters. From the data we obtain a diffusion exponent $m = 1.99$ by best linear fitting.

inset where we report the time dependence of the mean square displacement $\langle r^2(t) \rangle$ of the process for the same values of the control parameters in a log-log plot. By performing a best linear fitting of these data we obtain $m = 1.99$, in full agreement with previous numerical and theoretical investigations.[9] We study the time evolution of the probability distribution $P(r, t)$ after checking the presence of enhanced diffusion for each selected couple of control parameters. In Figs. 7 and 8 we show the time evolution of $P(r, t)$ obtained by setting $a = 3.75$ and $p = 0.5$. Figure 7 shows a linear plot of four $P(r, t)$ characterized by $t = 10, 30, 100$, and 300. From the figure it is hard to isolate the different curves; it is clear that the central peak remains almost constant in time over a very long period. In Fig. 8a we present the logarithm of the probability distributions obtained for the same values of the control parameters to point out the behavior of the wings of the probability distributions. From the plot we note that the probability is enhanced in the wings for longer times. Roughly speaking, we can state that this behavior is a manifestation on the distribution function of the observed enhanced diffusion of the variance of the process. In support of this qualitative statement, our simulation shows that the wings of the $P(r, t)$ distributions maintain their similarity in shape after a scaling performed by using

$$c^{m/2} P(c^{m/2} r, t) = P(r, t_1) \tag{12}$$

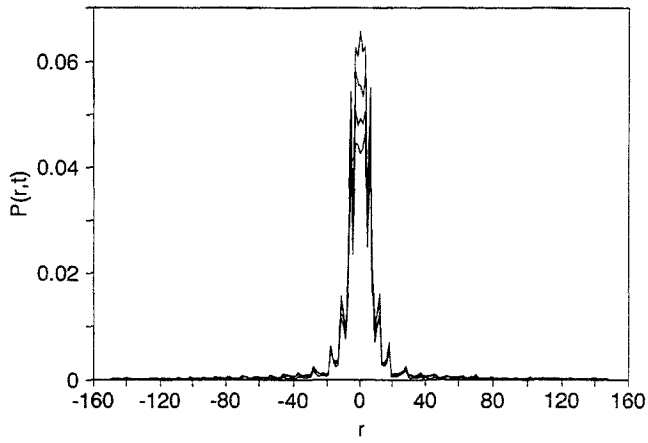

Fig. 7. Probability distributions for the amplified climbing-sine map ($a = 3.75$ and $p = 0.5$) obtained at different times ($t = 10$, 30, 100, and 300). The distributions are obtained by analyzing an ensemble of 5×10^4 different realizations. The probability distributions maintain almost the same shape for the investigated time intervals in the region close to the origin. In fact, except for the exact value at the origin, which decreases slowly, it is hard to resolve the four curves in the figure.

where $c = t/t_1$. It is worth noting either the formal analogy between Eq. (12) and Eq. (6) or the linear dependence of the scaling exponent $m/2$ on the diffusion exponent m. In Fig. 8b we present the same family of distributions already plotted in Fig. 8a by using the scaled units $r_s = r/t^{m/2}$ and $P_s(r_s, t) = t^{m/2}P(r_s, t)$. In addition to the curves plotted in Fig. 8a, in Fig. 8b we also plot the probability distributions obtained for $t = 1$, 3, and 10. In the scaling procedure, the scaling exponent $m/2$ is set to 0.995 as the diffusion exponent m, obtained by studying the time evolution of the mean square displacement of the process as show in the inset of Fig. 6, is equal to 1.99 for the selected values of the control parameters ($a = 3.75$ and $p = 0.5$). In the figure, after the scaling, the wings of the scaled distributions coincide, within the statistical errors, for $t \geqslant 10$. On the other hand, in spite of this, the central part of the probability distribution does not maintain similarity in shape after scaling (Fig. 7).

To summarize the results of this section, we state that the probability distributions of the amplified climbing-sine map are leptokurtic with a pronounced peak close to the origin and with wings which maintain similarity in shape after an appropriate scaling [Eq. (12)].

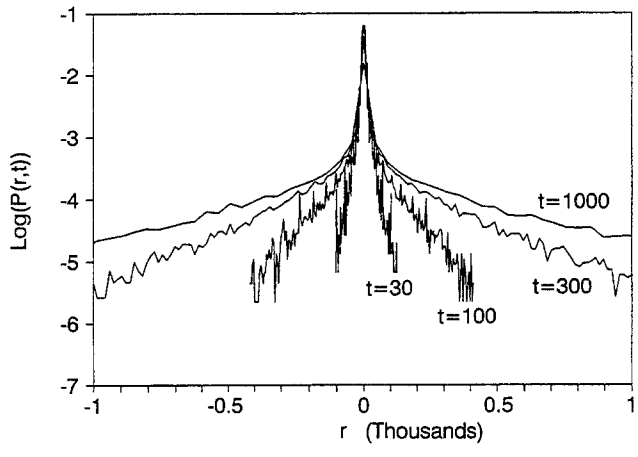

(a)

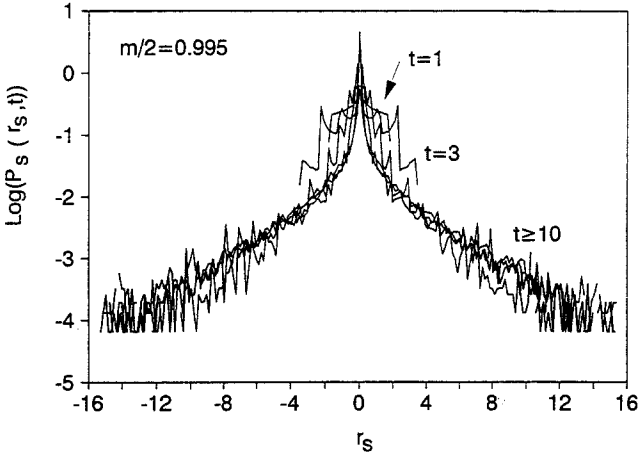

(b)

Fig. 8. Amplified climbing-sine map characterized by $a = 3.75$ and $p = 0.5$. (a) Logarithmic plot of the probability distributions obtained for different times ($t = 30$, 100, 300, and 1000). The wings of distributions are strongly enhanced for longer times. (b) The same probability distributions as in (a) with in addition the probability distributions obtained for $t = 1$, 3, and 10. In this plot the probability distributions are shown in the scaled units $r_s = r/t^{m/2}$ and $P_s(r_s, t) = t^{m/2}P(r_s, t)$. We use as scaling exponent the value $m/2 = 0.995$ because the diffusion exponent is equal to 1.99 for the selected values of the control parameters (Fig. 6). The wings of the scaled probability distributions coincide for $t \geqslant 10$, whereas the central part of the probability distribution does not show similarity after scaling.

4. DISCUSSION

In this last section we compare the two processes by pointing out analogies and differences. Both processes present a power-law time dependence for the time evolution of the mean square displacement. From this point of view both models could be used, for example, to model turbulence data. On the other hand, a detailed study of the probability distribution $P(r, t)$ shows differences. In particular, even if we set the control

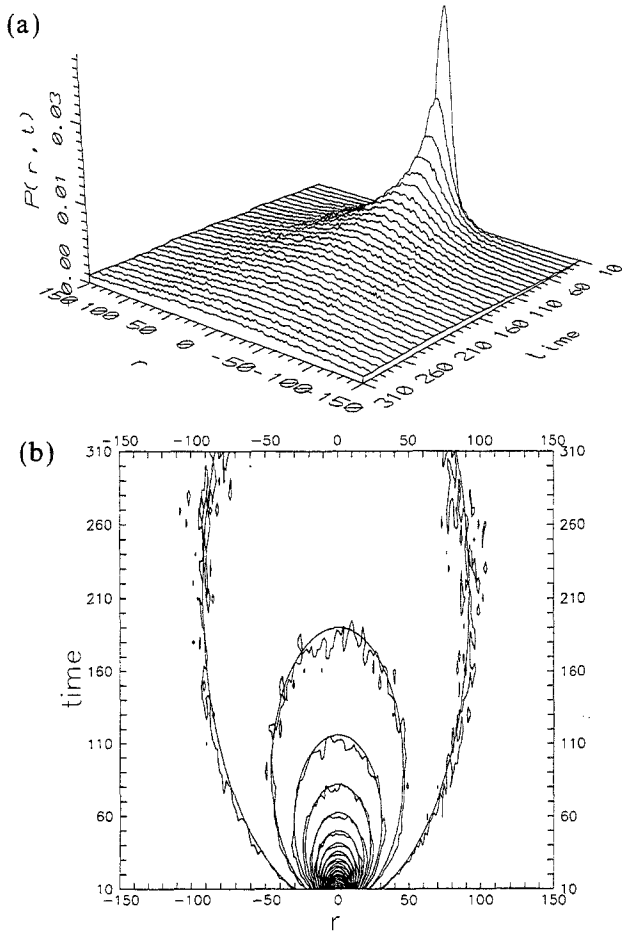

Fig. 9. One-dimensional Lévy walk ($\mu = 1.8$ and $\nu = 1.5$). (a) $P(r, t)$ investigated in the ranges $-150 \leqslant r \leqslant 150$ and $10 \leqslant t \leqslant 310$ (statistical ensemble of 5×10^4 realizations). In this figure all the scale units are the same as in Fig. 10a to allow a direct comparison between the two figures. (b) The contour line plot of the time evolution of $P(r, t)$. In the investigate spatial and temporal ranges the contour lines of simulations (noisy lines) are quite close to the contour lines of a Lévy flight distributions of order $\alpha = 1.22$ (smooth lines in the plot).

parameters to obtain nearly the same value of the diffusive exponent m for both processes [for example, $v = 1.5$ and $\mu = 1.8$ ($m = 2.05$) for the Lévy walk and $a = 3.75$ and $p = 0.5$ ($m = 1.99$) for the amplified climbing-sine map], the probability of returning to the origin $P(0, t)$ is completely different in the two cases. Moreover, a finer analysis of $P(r, t)$ shows that the difference is recognizable on a wide spatial region. In Figs. 9 and 10 we present the time evolution of the probability distributions $P(r, t)$ and the related contour line plots obtained for wide spatial and temporal ranges for a Lévy walk ($v = 1.5$ and $\mu = 1.8$) and for the amplified climbing-sine model ($a = 3.75$ and $p = 0.5$), respectively. In Figs. 9a and 10a we use the same scale for the z axis to allow a direct comparison of the two processes. It is evident that the behavior is deeply different in the two cases; for the Lévy walk we observe that the time evolution of the probability distribution is very close to the corresponding Lévy flight ($\alpha = 1.22$ obtained with the procedure sketched in Fig. 4) for the scanned spatial range, while the amplified climbing-sine map shows a strong central peak and a fine structure. The difference is even more evident if we analyze the contour lines for both simulations. For the Lévy walk (Fig. 10a) contour lines are closed loops passing through the origin and symmetric with respect to the time axis. Moreover, the contour lines of the process are quite close to the contour lines observed for the corresponding Lévy flights ($\alpha = 1.22$) in the investigated spatial ($-150 \leqslant r \leqslant 150$) and temporal ($10 \leqslant t \leqslant 310$) intervals (smooth lines in the figure). On the other hand, for the amplified climbing-sine map the contour lines are all parallel to the time axis in the same investigated intervals (Fig. 10b). This fine structure reveals the chaotic nature of the model.[25]

A further difference concerns the relation between the scaling and the diffusion exponents. For the amplified climbing-sine map the scaling exponent is found to be $m/2$ and then it is directly proportional to the diffusion exponent m. Lévy walks show a different behavior; in fact, for Lévy walks the two parameters are different and unrelated in the Lévy regime ($\alpha < 2$). We observe that the diffusion exponent m obtained from numerical simulations (Fig. 2) is close to the value

$$m = \begin{cases} 1 & \text{for} \quad \mu v > (1 + 2v) \\ 2 - \mu v + 2v & \text{for} \quad 1 + 2v > \mu v > 2 \\ 2v & \text{for} \quad 2 > \mu v > 1 \end{cases} \tag{13}$$

theoretically obtained in refs. 2 and 22, whereas the scaling exponent is equal to $1/\alpha$, i.e., is the inverse of the order of the Lévy distribution that well describes the central part of the probability distribution of the process. From numerical and theoretical investigations we know that $\alpha = \min((\mu v - 1)/v, 2)$ in the appropriate ranges of the control parameters

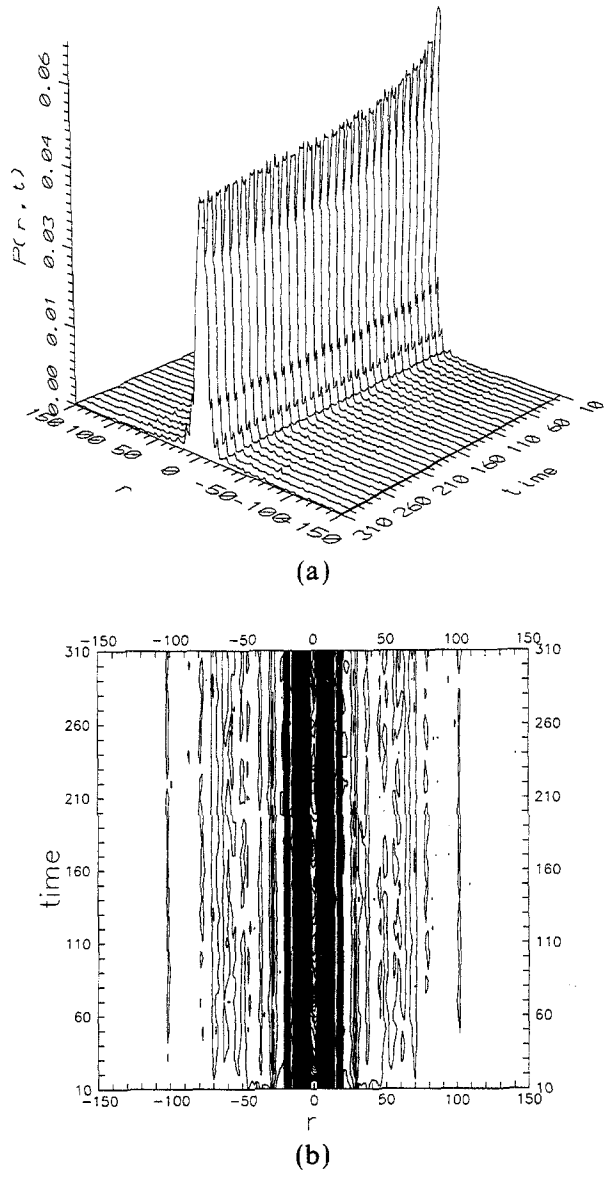

Fig. 10. Amplified climbing-sine map ($a = 3.75$ and $p = 0.5$). (a) $P(r, t)$ investigated for the same spatial and temporal ranges as for Fig. 9a (statistical ensemble of 5×10^4 realizations). The time evolution of $P(r, t)$ greatly differs from the one displayed for Lévy walks (Fig. 9a). It is leptokurtik, with a central peak slowly decreasing in time. (b) The contour line plot of $P(r, t)$. In this plot we observe that the contour lines are parallel to the time axis, a behavior completely different from the one observed in Lévy walks (Fig. 9b).

($\nu > 1/2$ and $\mu > 2/\nu$). By comparing Eq. (13) and Eq. (9) we can conclude that the diffusion and scaling exponents are related only in the Gaussian regime ($\alpha = 2$ and $m = 1$), where we can write $m/2 = 1/\alpha$, while in the Lévy regime ($\alpha < 2$ and $m \geqslant 1$) they are different and unrelated.

Our results on the shape of the central part of the probability distributions and on the relation between scaling and diffusive exponents for the two models show that it is possible to discriminate between the two models if one performs a careful examination of the time evolution of the probability distribution even for a set with a finite number of realizations of the process.

ACKNOWLEDGMENTS

The author is grateful to Prof. J. Klafter for fruitful discussions. Computer time was generously provided by the Centro Universitario di Calcolo of the University of Palermo. This work is supported in part by the Istituto Nazionale di Fisica della Materia.

REFERENCES

1. H. Scher and E. W. Montroll, *Phys. Rev. B* **12**:2455 (1975).
2. M. F. Shlesinger, J. Klafter, and Y. M. Wong, *J. Stat. Phys.* **27**:499 (1982).
3. E. W. Montroll and M. F. Shlesinger, in *From Stochastics to Hydrodynamics*, J. L. Lebowitz and E. W. Montroll, eds. (North-Holland, Amsterdam, 1984).
4. S. Havlin and D. Ben-Avraham, *Adv. Phys.* **36**:695 (1987).
5. J. P. Bouchaud and A. Georges, *Phys. Rep.* **195**:128 (1990).
6. W. Feller, *An Introduction to Probability Theory and Its Applications* (Wiley, New York, 1971).
7. O. Cardoso and P. Tabeling, *Europhys. Lett.* **7**:225 (1988).
8. I. Procaccia and H. Schuster, *Phys. Rev. A* **28**:1210 (1983).
9. A. Okubo, V. Andreasen, and J. Mitchell, *Phys. Lett.* **105A**:169 (1984).
10. T. Geisel, J. Nierwetberg, and A. Zacherl, *Phys. Rev. Lett.* **54**:616 (1985).
11. L. F. Richardson, *Proc. R. Soc. Lond. A* **110**:709 (1926).
12. M. A. Avellaneda, and A. J. Majda, *Commun. Math. Phys.* **131**:381 (1990).
13. A. Ott, J. P. Bouchaud, D. Langevin, and W. Urbach, *Phys. Rev. Lett.* **65**:2201 (1990).
14. R. N. Mantegna, *Physica A* **179**:232 (1991).
15. M. F. Shlesinger and J. Klafter, *Phys. Rev. Lett.* **54**:2551 (1985).
16. M. F. Shlesinger, B. J. West, and J. Klafter, *Phys. Rev. Lett.* **58**:1100 (1987).
17. P. Lévy, *Théorie de l'addition des Variables Aléatoires* (Gauthier-Villars, Paris, 1937).
18. B. B. Mandelbrot, *The Fractal Geometry of Nature* (Freeman, San Francisco, 1982).
19. B. B. Mandelbrot and J. W. van Ness, *SIAM Rev.* **10**:422 (1968).
20. G. Zumofen, J. Klafter, and A. Blumen, *J. Stat. Phys.* **65**:991 (1991).
21. G. Zumofen, A. Blumen, J. Klafter, and M. F. Shlesinger, *J. Stat. Phys.* **54**:1519 (1989).
22. A. Blumen, G. Zumofen, and J. Klafter, *Phys. Rev. A* **40**:3964 (1989).
23. E. W. Montroll and G. H. Weiss, *J. Math. Phys.* **6**:167 (1965).
24. V. Andreansen and A. Okubo, *Phys. Lett. A* **119**:117 (1986).
25. J. P. Eckmann and D. Ruelle, *Rev. Mod. Phys.* **57**:617 (1985).